COMBINATION OF SPECTRAL AND MULTI-RESOLUTION WAVELET ANALYSIS FOR FAULT DETECTION IN ELECTRIC MOTORS

Emine Ayaz Serhat Şeker Erdinç Türkcan
e-mail: ayaz@elk.itu.edu.tr e-mail: seker@elk.itu.edu.tr e-mail: eturkcan@elk.itu.edu.tr
İstanbul Technical University, Faculty of Electrical and Electronics Engineering,
Department of Electrical Engineering, 34469 Maslak, Istanbul, Turkey

Key words: Induction motors, Spectral analysis, Wavelet transform, Fault detection, Bearing damage

ABSTRACT

The purpose of this paper is to extract mechanical features from the motor current signals subjected to accelerated bearing fluting aging, and to detect the effects of bearing fluting at each aging cycle of induction motors. This feature of bearing degradation is achieved by monitoring the changes in the current signals at various sub-band levels. This is accomplished by the application of wavelet transforms and multi-resolution analysis (MRA) in order to extract information from selected frequency bands.

I. INTRODUCTION

The demand for monitoring and fault diagnosis of process dynamics and sensors in industrial systems has increased the efforts to develop new analysis techniques. The main goal of this technological improvement is to obtain more detailed information contained in the measured data than had been previously possible. Standard digital signal processing techniques, such as time series statistics, correlation analysis and fast Fourier transform (FFT), have been used to detect faults in system components [1-3].

Machinery that operates in a stationary mode are generally analysed with standard Fourier transform techniques. When a system is non-stationary or undergoes a transient, the Fourier technique does not provide proper information about the signals. The analysis of non-stationary signals should be performed using time-frequency (short-time Fourier transform, STFT) or time-scale (wavelet transform) techniques. The wavelet transforms can be used for localized analysis of signals continuously as a function of time. The discrete wavelet transform (DWT) permits a systematic decomposition of a signal into its sub-band levels. This can be performed with minimum distortion of the signal even for stationary signal analysis [3].

In literature, several studies have been conducted to identify the cause of failure of induction motors in industrial applications. More than fifty percent of the failures are mechanical in nature, such as bearing, balance and alignment related problems [4-8]. In this sense, the wavelet technique can be easily used to perform data analysis of rotating machinery under different operating conditions.

The paper presents a systematic approach to extract features from stator currents signals of 5-HP motors from load tests on motors subjected to bearing fluting or electrical aging. Test data are processed to assess the effect of bearing fluting in each aging cycle of the induction motor by using multi-resolution wavelet analysis methodology. As a result of this study, mechanical feature can be detected from the motor current signals by a new approach based on the wavelet analysis.

II. SPECTRAL ANALYSIS AND WAVELET TRANSFORM

In this section, combination of spectral analysis and multi-resolution wavelet analysis will be introduced. Hence a new approach based on sub band combination that defined in the frequency domain will be defined.

SPECTRAL ANALYSIS

A common approach for extracting the information about the frequency features of a random signal is to transform the signal to the frequency domain by computing the discrete Fourier transform. For a block of data of length N samples the transform at frequency $m\Delta f$ is given by

$$X(m\Delta f) = \sum_{k=0}^{N-1} x(k\Delta t)\exp\left[-j2\pi km/N\right]. \quad (1)$$

Where Δf is the frequency resolution and Δt is the data-sampling interval. The auto-power spectral density (APSD) of $x(t)$ is estimated as

$$S_{xx}(f) = \frac{1}{N}\left|X(m\Delta f)\right|^2,\ f = m\Delta f \quad (2)$$

The cross power spectral density (CPSD) between $x(t)$ and $y(t)$ is similarly estimated. The statistical accuracy of the estimate in Eq. (2) increases as the number of data points or the number of blocks of data increases [9].

WAVELET TRANSFORM AND MULTI-RESOLUTION ANALYSIS

The use of wavelet transform is particularly appropriate since it gives information about the signal both in frequency and time domains [10]. Let $f(x)$ be the signal, the continuous wavelet transform of $f(x)$ is then defined as

$$W_f(a,b) = \int_{-\infty}^{+\infty} f(x)\psi_{a,b}(x)dx. \tag{3}$$

Where

$$\psi_{a,b}(x) = \frac{1}{\sqrt{|a|}}\psi(\frac{x-b}{a}) \quad a,b \in R; a \neq 0 \tag{4}$$

ψ is called the mother wavelet and it has two characteristic parameters, namely, dilation (a) and translation (b), which vary continuously. Here, the translation parameter, "b", controls the position of the wavelet in time. A "narrow" wavelet can access high-frequency information, while a more dilated wavelet can access low-frequency information. This means that the parameter "a" varies for different frequencies. The parameters "a" and "b" take discrete values. $a = a_0^{\,j}$, $b = nb_0 a_0^{\,j}$, where $n, j \in Z$, $a_0 > 1$, and $b_0 > 0$. The Discrete Wavelet Transformation (DWT) is defined as

$$DWT[j,k] = \frac{1}{\sqrt{a_0^j}} \sum_n f[n]\psi\left[\frac{k - na_0^j}{a_0^j}\right] \tag{5}$$

S. Mallat introduced an efficient algorithm to perform the DWT known as the Multi-Resolution Analysis (MRA) [11]. The MRA is similar to a two-channel sub-band coder used in high-pass and low-pass filters, from which the original signal can be reconstructed.

Figure 1 shows the frequency decomposition of the signal schematically. The low-frequency sub-band is referred to as 'approximation a_i' and the high-frequency sub-band by 'detail d_i.' Thus, at the second stage the signal may be reconstructed as $S = a_2 + d_1 + d_2$.

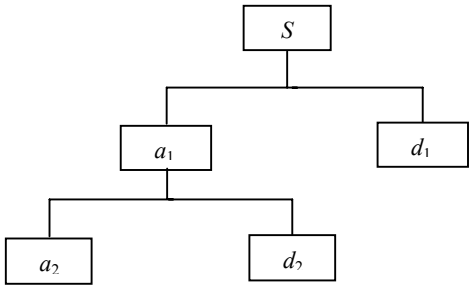

Figure1. Signal decomposition at the second stage.

COMBINATION OF APSD FUNCTIONS FOR SUB-BANDS

The signal reconstruction for sub-band analysis can be provided by the following equality.

$$y = c_n + \sum_{i=1}^{n} d_i \qquad n = 8 \text{ (in this application)} \tag{6}$$

Here, c_n and d_i's are indicate approximation and details from the sub-band analysis respectively. Hence, a new approach, which denotes the sub-band combination using the signal reconstruction defined in frequency domain, can be defined as below.

$$APSD\{y\} \triangleq APSD\{c_n\} + \sum_{i=1}^{n} APSD\{d_i\} \tag{7}$$

III. BEARING FLUTING MECHANISM AND EXPERIMENTAL SET UP

The rotor is supported by bearings with a grease film that is not conductive. At high speeds, an even distribution of the grease film exists, and the rotor is not in contact with the outer bearing race. The rotor voltage can increase with respect to ground. When this voltage builds to a level capable of breaking down the grease film, a spark occurs and discharge mode current flows through the bearing. At low speeds, the grease film is minimized. The balls often make contact with the race. The rotor voltage does not build. The current flows through the bearing in a conductive mode. The bearing current thus has two modes, conduction and discharge. Conduction mode bearing currents exhibit continuous flow through the bearings. This form of bearing current does not result in premature bearing failure because current flows continuously without arching. Discharge mode bearing currents occur at random when the grease film momentarily breaks down. When pits caused by the electric discharge machining effect continue to occur in an operating bearing and begin to overlap, groove-like configurations called "flutes" will form. This "fluting" is the source of audible bearing noise and reduced bearing life. As a result, rolling elements and the races get damaged. This surface degradation causes extreme

vibration levels of the bearing and its eventual failure. In order to simulate the electrical discharge from the shaft to the bearing, a special test set-up was designed. A schematic is shown in Figure 2. The fluting run had duration of 30 minutes with the motor rotating at no load, with an externally applied shaft current of 27 Amperes at 30 Volts AC. The fluting aging is followed by thermal and chemical aging in order to increase and accelerate the aging process. After each cycle of accelerated aging, the test motor was put on a motor performance test platform [12].

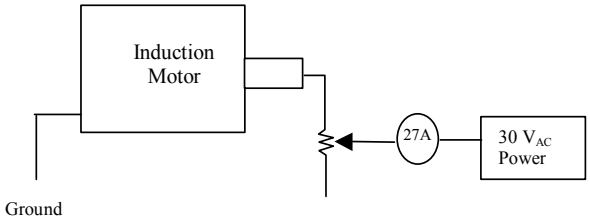

Figure 2. Electrical motor bearing fluting set-up.

IV. SIGNATURE ANALYSIS FROM MOTOR CURRENT SIGNALS

Motor aging study is performed on a 5-HP three-phase, four-pole induction motor. In this aging experiment, the test motor was failed at the end of seven aging cycles (final case). During these aging cycles there are a total of eight data sets, including the normal motor test data (initial case). Three motor current signals and six vibration signals from the normal condition and the final aging cycle tests were used for studying the effect of EDM on bearing degradation. These correspond to 100% load tests with a sampling rate of 12 kHz. In the signal condition unit, an anti-aliasing filter was set at 4 kHz. After the aging cycles, totally 8 data sets including the normal condition were used to analyse the motor current signals for one phase. For this aim, the waveform of the motor current signal related to the faulty case could be given by the following figure for a short time period of the total measurement time (10s). Also, the sub-band regions of one phase motor current were separated by the multi-resolution wavelet analysis as shown in Table 1.

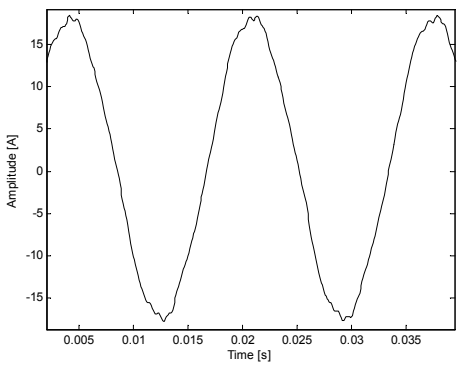

Figure 3. Waveform of stator current signal in final case.

Table 1. Sub-band intervals.

Approxi-mations (*a*)	Sub-bands (*a*) [Hz]	Details (*d*)	Sub-bands (*d*) [Hz]
*a*1	0 – 3000	*d*1	3000 – 6000
*a*2	0 – 1500	*d*2	1500 – 3000
*a*3	0 – 750	*d*3	750 – 1500
*a*4	0 – 375	*d*4	375 – 750
*a*5	0 – 187.5	*d*5	187.5 – 375
*a*6	0 – 93.75	*d*6	93.75 – 187.5
*a*7	0 – 46.88	*d*7	46.88 – 93.75
*a*8	0 – 23.44	*d*8	23.44 – 46.88

Wavelet function types, used for the multi-resolution analysis in separation of sub-bands, can be determined by means of the minimization of the energy function defined as Shannon's entropy function. Therefore, these function types are Daubechies-20 and Daubechies-15 for motor currents in healthy case and last aging case respectively [12]. Besides, in terms of the known spectral analysis techniques, the side-band effects of the motor current signals both of the healthy and faulty cases can be shown as given in Fig. 4a and 4b by means of their power spectral density variations at around supply frequency 60 Hz.

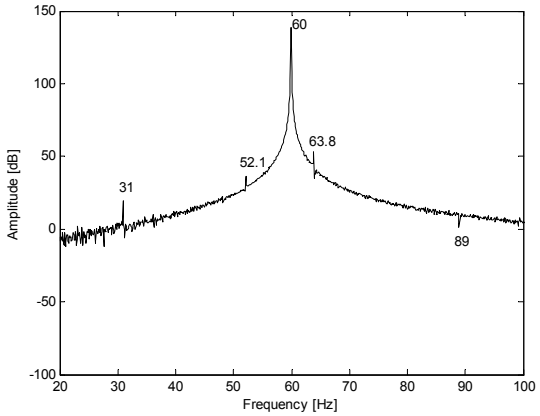

(a) APSD for healthy case.

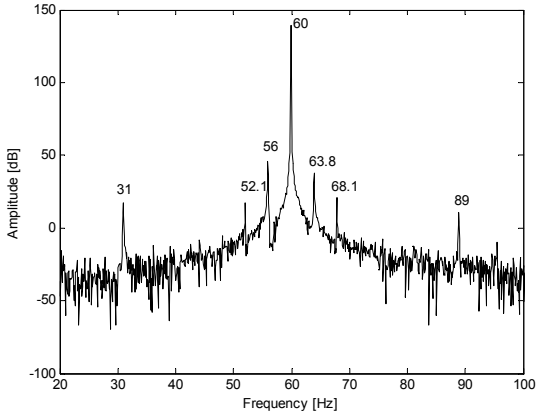

(b) APSD for aged case.

Figure 4. APSD variations for current signals

According to the above figures, the big amplitudes defined as side-band frequencies, which are appeared at around the fundamental frequency 60 Hz with difference of 4 Hz, indicate the rotor eccentricity. Here the side-band frequencies (f_{sb}) can be defined by the following equation [13,14]

$$f_{sb} = f_e\,(1 \pm 2\,k\,s) \tag{8}$$

Where f_e is the fundamental (supply) frequency, k is an integer and s is slip. In this application taking k=1,2 and s=0.032. From the Eq. (8), all side-band frequency values can be found at 52, 56, 64 and 68 Hz as shown in Fig. 5b. Also, comparing the Fig. 5a and 5b the other important frequency components can be determined at 31 Hz and 89 Hz. These are the rotor eccentricity frequencies and they can be defined between the rotational frequency (f_r) and fundamental frequency (f_e) as below [13,14].

$$f_{eec} = \left| f_e \pm k\,f_r \right|, \quad k=1,2,\ldots \tag{9}$$

where f_r is motor's rotating frequency. In this application it is f_r=1742/60=29.03 Hz.

In this sense, cause of the side bands occurred at around the fundamental frequency is rotor eccentricity or inhomogeneous magnetic field between rotor and stator. For example, a very small effect of the eccentricity appeared at 89 Hz for initial case is forced as a result of the degradation of motor bearing in final aged case and it causes to a new side-band component at 68 Hz. In this manner, there is highly correlation between the side bands and eccentricity frequencies. Hence, these eccentricity frequencies, namely 31 and 89 Hz, can be defined as most dominate mechanical features hided in stator currents.

Using the Heisenberg's uncertainty principle that defined in spectral analysis, if the frequency resolution is decreased then side-band amplitudes can be removed from the original spectra and all peaks related to the eccentricity frequencies are forced by using the new approach, which is based on the sub-band combination in frequency domain. To show this property, considering the total range of 0-6 kHz, the frequency resolution is computed as Δf = 6000/60000 =0.1 Hz for overall data length, whereas, to show the eccentricity effects ignoring the side-bands, new resolution (Δf^*) can be chosen as Δf^*>0.1 Hz, hence it can be determined as Δf^*=2.92 Hz for FFT block of length N=4096 samples. Within this resolution limit (Δf^*=2.92 Hz), the first eccentricity frequency, 31±2.92 Hz can overlap with the motor shaft's rotating frequency (29.03±2.92 Hz) and other eccentricity frequencies related to the 31±2.92 Hz are defined with the frequencies of 127.84 and 195.68 Hz using the Eq.(9) as shown in the Fig.5. For this case, Fig.5 reflects the all peak amplifications occurred at eccentricity frequencies like 33.92, 127.84 and 195.68 Hz.

This event is shown with the following figure.

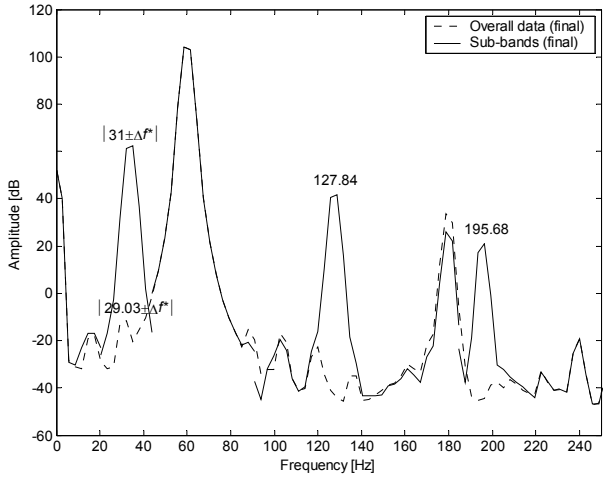

Figure 5. Original spectrum and spectrum of sub-band combination for motor current signal in final aged case.

V. CONCLUSIONS AND DISCUSSIONS

Using the new approach, which is defined by the sub-band combination in frequency domain, it is easily observed the effect of the eccentricity frequency values that detected from the spectral variation of the sub-band combination. Also, this amplified effects correlated with the rotating frequency can be related to bearing damage problem in the physical sense. In this manner, this proposed method could be interpreted as a new approach for fault detection problem related to the mechanical feature by means of the electrical quantities such as motor current signals.

ACKNOWLEDGMENT

Authors wish to express their appreciations to Prof. Dr. B. R. Upadhyaya from the University of Tennessee, Nuclear Engineering Department.

REFERENCES

1. S. Şeker, E. Ayaz, A Study on Condition Monitoring for Induction Motors Under the Accelerated Aging Processes, IEEE Power Engineering Review, Vol. 22, Issue 7, July 2002.
2. S. Şeker, E. Ayaz, A Reliability Model for Induction Motor Ball Bearing Degradation, Electric Power Components & Systems, Vol. 31, No. 7, July 2003.
3. S. Şeker, E. Ayaz, Feature Extraction Related to Bearing Damage in Electric Motors by Wavelet Analysis, Journal of the Franklin Institute, Vol.340, Issue 2, March 2003, pp. 125-134.
4. R.R. Schoen, T.G. Habetler, F. Kamran and R.G. Bartheld, Motor Bearing Damage Detection Using Stator Current Monitoring, IEEE Transactions on Industry Applications, 31, No.6, 1274-1279, 1995.
5. R.R. Schoen et al., An Unsupervised, On-Line System for Induction Motor Fault Detection Using

Stator Current Monitoring, IEEE Transactions on Industry Applications, 31, No.6, 1280-1286, 1995.
6. E. Ayaz, Bearing Fault Diagnosis with the Approach of Wavelet Analysis and a Condition Monitoring System Based on Artificial Intelligence in Electric Motors, PhD Thesis-İTÜ Institute of Science and Technology, May 2002.
7. H. Prashad, Diagnosis and Cause Analysis of Rolling-Element Bearing Failure in Electrical Power Equipment Due to Current Passage, Lubrication Engineering, May, 30-35, 1999.
8. S. Şeker, E. Ayaz, B.R. Upadhyaya, A.S. Erbay, Analysis of Motor Current and Vibration Signals for Detecting Bearing Damage in Electric Motors, MARCON 2000, Maintenance And Reliability Conference, Knoxville, May 8-10, 2000.
9. V.S. Vaseghi, Advanced Signal Processing and Digital Noise Reduction, John Wiley, New York, 1996.
10. I. Daubechies, The Wavelet Transform, Time-Frequency Localization and Signal Analysis, IEEE Trans. on Information Theory, 36, No.5, 1990.
11. S. Mallat, A Theory for Multiresolution Signal Decomposition the Wavelet Representation, IEEE Trans. Pattern Anal. And Machine Intelligence, 11, No.7, 674-693, 1989.
12. S. Şeker, B.R. Upadhyaya, A.S. Erbay, J.P. McClanahan and A.A. daSilva, Rotating Machinery Monitoring and Degradation Trending Using Wavelet Transforms, Maintenance and Reliability Conference Proceedings, 1, pp. 23.01-23.11, 12-14 May, Knoxville, 1998.
13. O.V. Thorsen, M. Dalva, Methods of Condition Monitoring and Fault Diagnosis for Induction Motors, ETEP, 8, No. 5, 383-395, 1998.
14. D. Rankin, The Industrial application of phase current analysis to detect rotor winding faults in squirrel cage induction motors, Power Engineering Journal, April, 77-84, 1995.